Heliyon 7 (2021) e08241

Contents lists available at ScienceDirect

Heliyon

journal homepage: www.cell.com/heliyon

Review article

Harbor and coastal structures: A review of mechanical fatigue under random wave loading

Moises Jimenez-Martinez *

Tecnologico de Monterrey, Escuela de Ingeniería y Ciencias, Via Atlixcayotl 5718, Col. Reserva Territorial Atlixcayotl, C.P. 72453 Puebla, Mexico

ARTICLE INFO

Keywords:
Coastal
Mechanical fatigue
Damage
Harbor
Random processes

ABSTRACT

Harbor and coastal structures are essential in maritime connections. Additionally, some offshore structures near the coast are important for supplying energy as a material or transforming the natural resources into energy, as in wind turbines. One of the main issues that needs to be overcome in terms of these structures is mechanical fatigue due to the loads of the structure by its function and waves, wind, the current seawater level, and ice. Structural design has to meet high target loads to ensure that structures can endure extreme marine conditions under the assumption of the probability of loads and based on marine conditions, can mask damage where component immersions are not available for inspection. In this work, the wave loads and fatigue damage under random processes are reviewed.

1. Introduction

Coastal structures are located on the shore or near the coast (sea dikes, sea walls, bulkheads, groynes, jetties, break water), and involve coastal modeling at depths greater than 20-50 m and locations 50-100 km from the shore. A port is a location on a coast or shore containing harbors where ships can dock and transfer. A harbor is a sheltered area of the sea in which vessels can be launched, built, or repaired [1, 2]. To include waves effect, a sea state is used integrating its parameters as period and height, including the wind, water levels and wave transformation considering fluctuations due to storms. In coastal engineering models considers information from the current (tidal, wind-driven, wave-driven currents, hydrographic data, sediment (gravel, sand, silt, or clay), data erosion (alongshore, cross-shore), and sediments which are a mixture of sand and gravel. Fig. 1 presents a simple coastal subsystem.

Based on the high mechanical stresses generated in offshore structures, these designs require a high reliability common evaluated in an annual probability to prevent failures as cracks [3, 4, 5, 6]. Wave heights distribution depends on the physical phenomenon associated with it; for example, monsoonal extremes are different from extremes in typhoons [7, 8, 9]. Standardized wave load histories known as *WASH* (Wave Action Standardized History), combine load aspects and sea state considerations [10]. Offshore wind farms could become an important source of energy due to it has higher capacity than onshore. Monopile

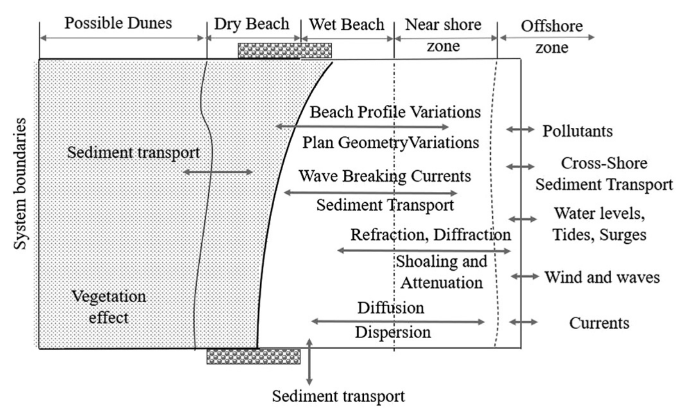

Fig. 1. Coastal subsystem.

Offshore Wind Turbines *OWTs* are frequently subjected to unexpected loads [11, 12, 13] (see Fig. 2), it can reduce its fatigue life in deeper regions due to flow-structure interaction [14, 15], it also happens in flexible risers [16, 17] dampers can be used to reduce load amplitude controlling the oscillations [18].

Rubbers in a marine environment have to be designed to be used in marine environment [19]. Environmental effects reduce the material properties due to wave climate change and marine corrosion [20, 21, 22, 23], pitting corrosion is the most dangerous [24]. In a very high cycle fatigue region for martensitic-bainitic hot rolled steel the main fatigue process is by corrosion [25], this is a time-dependent mechanism. Although corrosion protection mechanism as cathodic protection

* Corresponding author.
E-mail address: moisesjimenezmartinez@gmail.com.

https://doi.org/10.1016/j.heliyon.2021.e08241
Received 17 August 2021; Received in revised form 4 October 2021; Accepted 20 October 2021

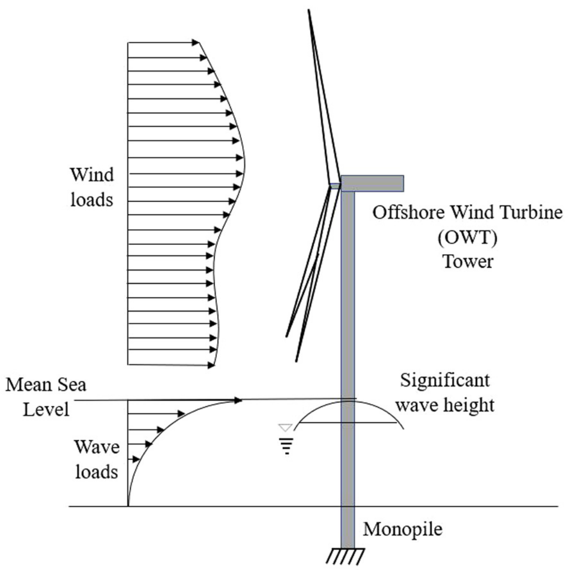

Fig. 2. Offshore Wind Turbine (OWT) model under loads.

or surface coating is applied on parts in contact with seawater, it can be damaged or wear by structure operation or external impacts [26], to prevent it, the structure deformation mechanism has been analyzed in marine structures [27, 28, 29, 30]. To minimize its effect on structure strength and corrosion protection, foamed metals can be used in marine structures due to its ability to absorb impact energy [31]. Liu et al. [32] proposed a crashworthy design to monopile foundation of OWTs. Thickness has an effect to enhance the cathodic polarization due to differences in plasticity between the outside and inside components [33], the corrosion mechanism can be modified by temperature increase accelerating the crack growth [34]. The cathodic protection depends on applied loads and potential for T-joints of a quenched and tempered steels [35]. In seawater, the mean stresses have an effect on crack propagation [36, 37]. Cheng and Chen [38] proposed a corrosion-crack model to improve the Engineering critical assessment for structures in seawater.

Chang et al. [39], proposed a fatigue estimation methodology using Dynamic Bayesian Network for subsea wellheads. Additionally, Piedras Lopes and Ebecken [40] proposed a process to monitor the fatigue on fixed components. The cumulative fatigue damage induced by vortex-induced vibration is determined using the Palmgren Miner rule [41]. Numerical tools can be implemented to improve fatigue prediction for wide-bands using Artificial Neural Network (*ANN*) [42]. Machado et al. [43] proposed a spectral shaker model for fatigue assessment. Linear damage rule is used in the design of maritime structures, and relates material properties to the loads to evaluate the mechanical fatigue strength [44, 45]. To review the phenomenological effect of fatigue in coastal and harbor structures, this work is organized based on concepts in harbors, waves, and fatigue prediction under a random process.

2. Geometry of the harbor region

In a harbor region, the fluid domain is split into a harbor (bounded) region, an unbounded region, and a ship region, as is shown in Fig. 3.

The form of the velocity potential is

$$\phi(x,y,z,t) = -\frac{ig}{\omega} f(x,y)\, Z(z)\, e^{-i\omega t} \tag{1}$$

where ω is an angular wave frequency and $Z(z)$ is the depth function. The wave function f_b at point (x,y) inside the harbor is

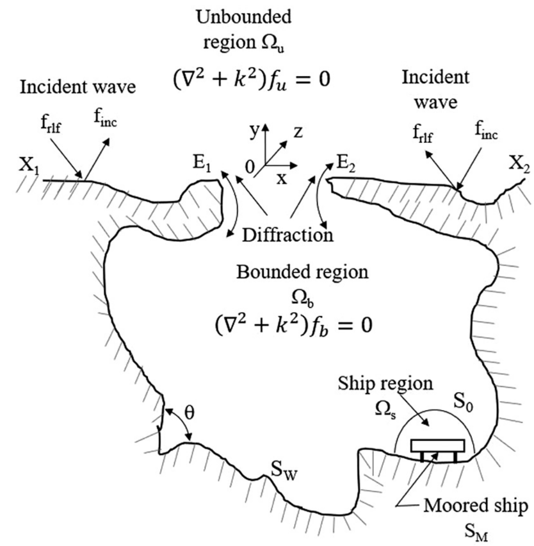

Fig. 3. Schematic model in a moored ship.

$$f_b(x,y) = C \int_{S_W} \left\{ f_b(x_0,y_0) \frac{\partial}{\partial n} H_0^1(kr) - H_0^1(kr) \frac{\partial}{\partial n} f_b(x_0,y_0) \right\} ds(x_0,y_0) \tag{2}$$

where S_W is the harbor boundary [46].

3. Wave description

Waves are changes of the water level, which depend on the wind's interaction with the gravity force. They can be represented by a simple form of sinus [47].

A wave description depends on systems (wind sea and swells). The significant wave height is represented by H_s and the spectral wave period is represented by T_p (T_z) [48] (Fig. 4). Wave spectra can be represented by their spectral moment M_n

$$M_n = \int_{-\infty}^{\infty} \omega_e^n S(\omega)\, d\omega \tag{3}$$

where ω_e is the wave encounter frequency, spectral moment of order n = 0 is the displacement, n = 2 is the velocity and n = 4 is the acceleration. The fatigue damage is [3]:

$$D = \frac{T\omega_{z\sigma}}{K} \left(2\sqrt{2M_0}\right)^m \Gamma(1+m/2) \tag{4}$$

where $\omega_{z\sigma}$ is the zero-crossing frequency of the load, T is the time at sea, m and K are mechanical properties parameters

The spectrum for sea state generated by wind is given by directional wave as

$$S_\eta(\omega,\theta) = S_\eta(\omega)\, D(\omega,\theta) \tag{5}$$

The effects among current velocity $\dot{v}_c$, fluid (water density ρ), and structure velocity $\dot{u}$ is

$$p_h = C_m \rho \cdot V_p \ddot{v} + \frac{1}{2} C_d \rho A_p \left(\dot{v} + \dot{v}_c - \dot{u}\right) \left|\dot{v} + \dot{v}_c - \dot{u}\right| \tag{6}$$

where C_d is the drag coefficient and C_m is inertia coefficient.

The vertical bending stress, $RAO_{\sigma,ver}$ is

$$RAO_{\sigma,ver} = SCF \cdot \frac{z - z_0}{I_{yy}} RAO_{M,ver} \tag{7}$$

where the vertical distance from the baseline is z for the vertical distance from the structural detail and z_0 from the neutral axis.

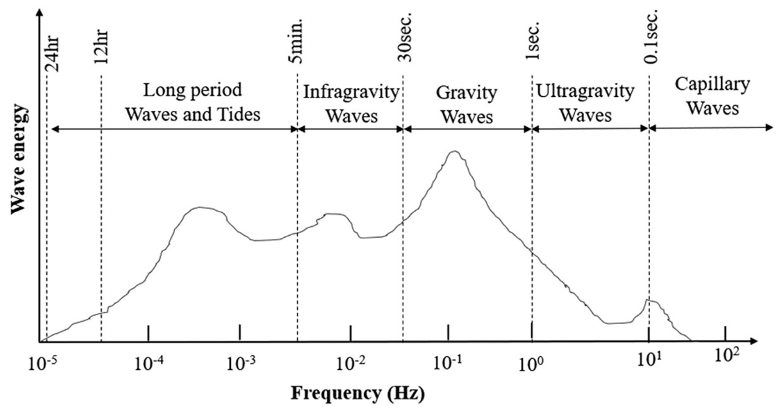

Fig. 4. Wave classification by frequency.

The stress transfer function, $H_\sigma(\omega|\theta)$, is used to get:

$$S_\eta(\omega|H_s,T_z,\theta)=\left|H_\sigma(\omega|\theta)\right|^2 S_\eta(\omega|H_s,T_z) \tag{8}$$

where the spectral moments (μ_n), of the response process are expressed by

$$\mu_n=\int_\omega \sum_{\theta-\pi/2}^{\theta+\pi/2} f_s(\theta')\cdot\omega^n S_\sigma(\omega|H_s,T_z,\theta)\,d\omega \tag{9}$$

The single moment spectral method is useful for predicting fatigue life in offshore structures under random loads, other used spectral methods are: Wirsching and Light, Zhao and Baker, Steinberg three-band method, Fu-Cebon, Gao and Moan, and Lalanne. [49, 50, 51]. On ship structures the load response (Fs_{ij}) is

$$Fs_{ij}(\Delta\sigma_k)=1-exp\left(\frac{\Delta\sigma_k^2}{8\mu_{0,ij}}\right) \tag{10}$$

$$f_{0,ij}=\frac{1}{2\pi}\sqrt{\frac{\mu_{2,ij}}{\mu_{0,ij}}} \tag{11}$$

Therefore, based on the linear damage rule its durability assessment can be evaluated by

$$D=\sum_{k=1}^{n_b}\frac{n_k}{N_k}=\frac{N_d}{A_\alpha}\int_0^\infty(\Delta\sigma_k)^{m_\alpha} f_\sigma(\Delta\sigma_k)\,d\Delta\sigma=\frac{N_d}{A_\alpha}E\left[(\Delta\sigma_k)^{m_\alpha}\right] \tag{12}$$

The cumulative damage for a one-slope can be evaluated with eq. (13) and for a S-N curve with two slopes with eq. (14) [44, 52]:

$$D=\frac{\nu_0 T_d}{A_1}\sum_{x=1}^{n_x} r_x q_x^{m_1}\Gamma\left(1+\frac{m_1}{h_x}\right) \tag{13}$$

$$\begin{aligned}D=&\nu_0 T_d\sum_{x=1}^{n_x} r_x\left\{\frac{q_x^{m_1}}{A_1}\Gamma\left[1+\frac{m_1}{h_x};\left(\frac{\Delta\sigma_{slope}}{q_x}\right)^{h_x}\right]\right.\\&\left.+\frac{q_x^{m_2}}{A_2}\gamma\left[1+\frac{m_2}{h_x};\left(\frac{\Delta\sigma_{slope}}{q_x}\right)^{h_x}\right]\right\}\end{aligned} \tag{14}$$

where n_x is the total number considered load cases and $\Delta\sigma_{slope}$ is the stress range at which the slope changes.

4. Fatigue

Mechanical fatigue is a phenomenological process where the material strength is degraded for stresses [53], its analysis is important in structural components under irregular loads generated by rough roads, waves and wind. Fatigue failure is reached when the damage attained from the loads degrades the life in an accumulated process [54, 55, 56].

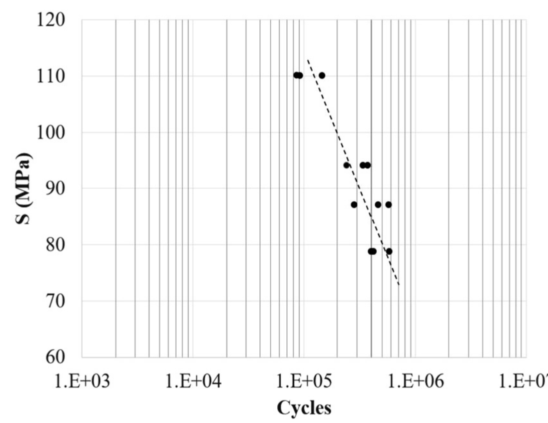

Fig. 5. SN curve for aluminum.

Fig. 6. Uniaxial fatigue test.

The evaluation of fatigue load histories is analyzed by cycle counting methods, in which repetitions for different load amplitudes are represented. Fatigue load resistance is evaluated using SN curves, also known as *Wöhler* curves. These fatigue strength properties represent the strength of the material characterized by tests on standard samples, as shown in Fig. 5. These S-N curves of the material are obtained by test equipment as shown in the Fig. 6.

S-N curves also represent the behavior of the component under operating conditions, this allows analysis of the effect of manufacturing processes Fig. 7. For evaluation, durability tests are developed with the aim of reproducing cyclic load failures in an accelerated manner. Fig. 8

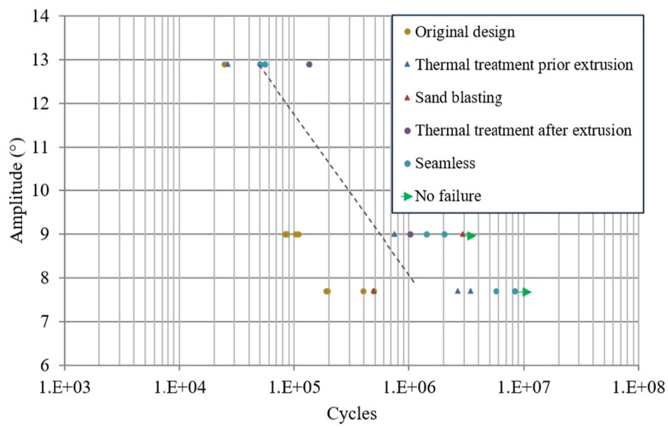

Fig. 7. Component S-N curve.

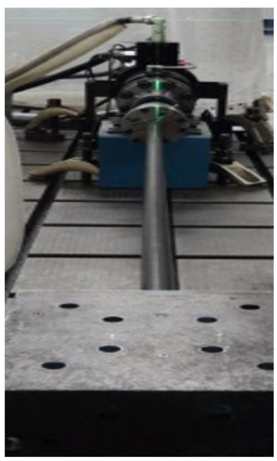

Fig. 8. Torsional component test.

shows a test bench for evaluation of a component under torsional load [57].

Mechanical fatigue analysis is performed to prevent unexpected failures during product service, during which loads not only come from its operation, but are also generated by high-temperature and aggressive environments [58, 59, 60, 61], some areas don't have an easy access it has to support high number of cycles, it is in the very high cycle region [62, 63, 64, 65]. Zalaznik and Nagode [66] proposed a modified Dirlik method to evaluate fatigue damage at elevated temperature in high cycle region. The load frequency can affect the mechanical behavior, which has been investigated by heat generation [67, 68, 69, 70, 71]. In pipelines, fluid temperature changes cause stress fluctuations resulting in damage, which reduce its structural integrity and can lead to leakage [72]. The waveform, load ratio, and hold time also have a fatigue effect [65, 73, 74, 75].

Fatigue analysis has evolved depending on the equipment available to analyze it. In closed-loop fatigue evaluation, it is possible to monitor the damage directly with the measurements of fatigue feedback, meaning when the control is displacement the feedback is force or if the control is force the feedback is the displacement. Another approach is to monitor the stiffness by evaluating stiffness change during the test [76, 77, 78]. The fatigue limit analyzed with high frequency equipment change depending on the material evaluated [68, 79, 80, 81, 82, 83], the component area as in welds [84, 85, 86, 87, 88].

The material or component fatigue strength is represented by the SN curve; this curve is mostly represented by a line due to its log-log scale, as started in the 1850s by *Wohler* [54, 89]. To analyze the mechanical damage or fatigue generated by the loads, counting methods are used,

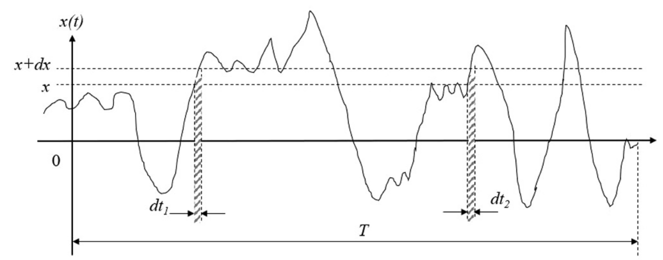

Fig. 9. Probability density function p(x) for a random process.

this can take a long process to obtain reliable results. Zhao and Baker [90] proposed a model for the probability distribution of the rainflow stress range using only spectral properties. Although a fatigue limit has been considered, there are failures after this hypothetical limit. The failure origin can change from the external area (surface) to the interior [64, 65, 91]. However, most research has been conducted on High Cycle Fatigue (*HCF*). An evaluation of the scatter showed the accuracy and reliability of the fatigue evaluation, as well as the production process [55, 92]. Failures after the theoretical fatigue limit have been found [93]. The increase in temperature can be used to detect a damage [62, 94], and the dynamic modulus might prove to be a valuable indicator of the degree of fatigue damage [95, 96].

The scatter in the prediction of mechanical fatigue comes from the variability of the material, the manufacturing processes, unexpected loads, and the environment. Fatigue predictions using frequency domain techniques are more efficient than time-domain predictions [51].

4.1. Fatigue analysis under a random process

Loads whose outcome at a future instant cannot be predicted are classified as nondeterministic (random), which are the result of a stationary process, for these loads are used the power spectral density (PSD) [97]. To classify the random signals $s(t)$ the form of the PSD is used if the circular frequency function $G(\omega)$ has a peak around a single frequency, it is a narrow band. In cases where the PSD has more peaks it can be defined as bimodal, trimodal or multimodal, usually known wide band process [51]. Its probability function is expressed by

$$P(S) = \frac{\frac{D_1}{Q} e^{\frac{-Z}{Q}} + \frac{D_2 Z}{R^2} e^{\frac{-Z^2}{2R^2}} + D_3 Z e^{\frac{-Z^2}{2}}}{\sqrt{m_0}} \tag{15}$$

where

$$D_1 = \frac{2\left(x_m - \gamma^2\right)}{1+\gamma^2} \cdot D_2 = \frac{1-\gamma-D_1+D_1^2}{1-R} \cdot D_3 = 1 - D_1 - D_2 \cdot Z = \frac{S}{\sqrt{m_0}} \tag{16}$$

$$Q = \frac{1.25\left(\gamma - D_3 - D_2 R\right)}{D_1} \cdot R = \frac{\gamma - x_m - D_1^2}{1-\gamma-D_1+D_1^2} \cdot \gamma = \frac{m_2}{\sqrt{m_0 m_4}} \cdot x_m = \frac{m_1}{m_0}\sqrt{\frac{m_2}{m_4}} \tag{17}$$

While in deterministic loads Fig. 9 are used the mean values of loads, in random process is used the ensemble $E[x]$ to mathematically calculate the average. If statistical properties such as the mean standard deviation and the mean square properties are the same along with any sample across the time history ensemble, the process is called ergodic. The area under the x(t) curve in the interval T is

$$E[x] = \int_0^T x(t)\,\frac{dt}{T} \tag{18}$$

To consider all the effects on the response, different measures $x_1(t)$, $x_2(t)$, $x_3(t)$, $x_1(t)$, $x_4(t)$ to get the behavior of t_1, t_2, t_n these measures are used to analyze the random process as is shown in Fig. 10

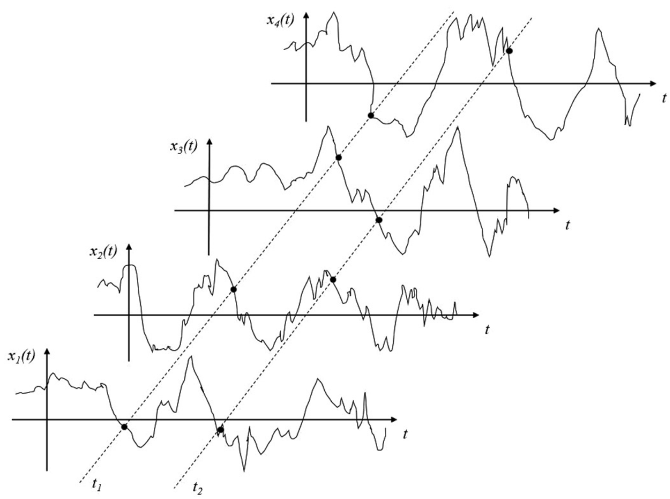

Fig. 10. Ensemble averaging.

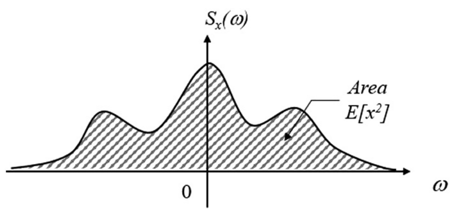

Fig. 11. Area under spectral density.

Ensemble averages are evaluated with the autocorrelation function $R_x(\tau)$ through the average value of $x(t)\,x(x+\tau)$. $R_x(\tau)$ gives information about the frequencies in a random process indirectly, it is related with the spectral density $S_x(\omega)$ of the amplitude x and is function of angular frequency ω

$$R_x(\tau)=\int_{-\infty}^{\infty} S_x(\omega)\,e^{i\omega\tau}d\omega \tag{19}$$

The area under a graph of the mean square spectral density $S_x(\omega)$ against ω is $E\left[\omega^2\right]$

$$S_x(\omega)=A(\omega)-i\,B(\omega) \tag{20}$$

where

$$A(\omega)=\frac{1}{2\pi}\int_{-\infty}^{\infty} R_x(\tau)\,cos\omega\tau\,d\tau \tag{21}$$

$$B(\omega)=\frac{1}{2\pi}\int_{-\infty}^{\infty} R_x(\tau)\,sin\omega\tau\,d\tau \tag{22}$$

As is shown in Fig. 11, $S_x(\omega)$ is real and non negative function of ω, so that $B(\omega)$ is therefore zero and $S_x(\omega)=A(\omega)$.

The time history shown in Fig. 12 is an schematic representation of a narrow band process.

Its spectral density is shown in Fig. 13, the frequencies only occupy a narrow band.

The second order probability density function $p(y,\dot{y})$ for the joint probability y and its derivative $\dot{y}$.

In the time history for a broad band process when $\omega_1\approx 0$ and $\omega_2\approx 0$ the spectrum is called white. When $\omega_1=0$, $R_x(\tau)$ is defined by

$$R_x(\tau)=\frac{4S_0}{\tau}cos\frac{\omega_2\tau}{2}sin\frac{\omega_2\tau}{2}=2S_0\frac{sin\omega_2\tau}{\tau} \tag{23}$$

When $\omega_2\rightarrow\infty$ the response becomes a vertical spike with zero width, infinite height and the area reach the magnitude $2\pi S_0$.

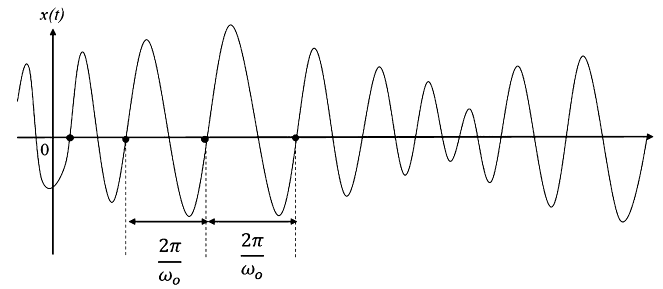

Fig. 12. Time history from a narrow band process.

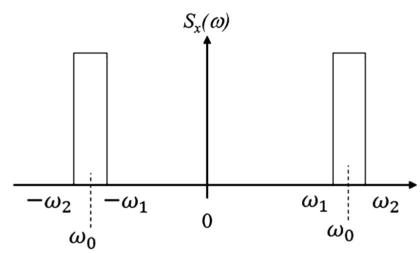

Fig. 13. Spectral density from a narrow band process.

For non constant loads, the damage (D) is

$$D=\frac{\sum_{i=1}^{k}n_i}{A}\sum_{i=1}^{k}f_iS_{a,i}^m \tag{24}$$

Additionally, the expected value of S_a^m is

$$E\left(S_a^m\right)=\sum_{i=1}^{k}f_iS_i^m \tag{25}$$

Therefore,

$$D=\frac{\sum_{i=1}^{k}n_i}{A}E\left(S_a^m\right) \tag{26}$$

If S_a can be evaluated as a continuous random variable. Its expected value is [98]

$$E\left(S_a^m\right)=\int_{0}^{\infty}S_a^m f S_a\left(S_a\right)dS_a \tag{27}$$

for S(t) stationary [41].

$$E\left(S_a^m\right)=\left(\sqrt{2}\sigma_s\right)^m\Gamma\left(\frac{m}{\beta}+1\right) \tag{28}$$

where $\sigma_s=\sqrt{M_0}$. The expected total fatigue damage under a narrow-band random process D_{NB} is represented as

$$D_{NB}=\frac{\sum_{i=1}^{k}n_i}{A}E\left(S_a^m\right)=\frac{E\left[0^+\right]\times T}{A}\left(\sqrt{2M_0}\right)^m\Gamma\left(\frac{m}{2}+1\right) \tag{29}$$

The damage $(D_{WB,Wirshing})$ is

$$D_{WB,Wirsching}=\zeta_w D_{NB} \tag{30}$$

where ζ_w is the rainflow correction factor. *Oritz* and *Chen* proposed a damage approach for a wide-band stress as

$$D_{WB,Oritz}=\zeta_0 D_{NB} \tag{31}$$

where

$$\zeta_0=\frac{1}{\gamma}\sqrt{\frac{M_2M_k}{M_0M_{k+2}}} \tag{32}$$

An approach for the Rainflow amplitude $f_{Sa}(S_a)$ [99, 100], is expressed by Dirlik damage model eq. (33) and the amplitude is described in equation (34):

$$D_{WB,Dirlik} = \frac{E[P]\tau}{A}\int_0^{\infty} S_a^m f S_a(S_a)\, dS_a \tag{33}$$

$$F_{Sa}(S_a) = \frac{D_1}{2\sqrt{M_0}Q}e^{-\frac{Z}{Q}\times S_a} + \frac{D_2\times Z}{2\sqrt{M_0}R^2}e^{\frac{-Z^2}{2R^2}\times S_a^2} + \frac{D_3\times Z}{2\sqrt{M_0}}e^{\frac{-Z^2}{2}\times S_a^2} \tag{34}$$

where

$$Z = \frac{1}{2\sqrt{M_0}}, \gamma = \frac{M_2}{\sqrt{M_0 M_4}}, Xm = \frac{M_1}{M_0}\sqrt{\frac{M_2}{M_4}}, R = \frac{\gamma - X_m - D_1^2}{1-\gamma-D_1+D_1^2} \tag{35}$$

where (γ) is an irregularity factor, that is a measure of the fluctuation of the load with its mean load and X_m is the mean frequency [101].

Fatigue damage that corresponds to a period of T [40]is:

$$D_T = \frac{T\sqrt{\frac{M_4}{M_0}}\left(\frac{\varepsilon^{m'+2}}{2\sqrt{\pi}}\Gamma\left(\frac{m'+1}{2}\right) + \frac{3\alpha}{4}\Gamma\left(\frac{m'+2}{2}\right)\right)\left(2\sqrt{2M_0}\right)^{m'}}{A_{SN} f_c^{m'}} \tag{36}$$

Due to the random process involved in fatigue, a probabilistic method can be used [102]:

$$\int_{a_0}^{a_N} \frac{da}{GY^m(\pi a)^{0.5m}} = C\bar{\lambda}^m SCF^m \bar{S}^m N \tag{37}$$

where the initial crack depth is a_0, a_N is the cumulative crack depth and λ^m is overloading history.

4.2. Artificial Neural Network in fatigue life assessment

Artificial Neural Networks (ANN) are considered artificial intelligence modeling techniques for complex models only using the study's data. It has interconnected neurons as in the human brain. Each structure or neuron can be connected to another neuron in the next layer and has a relationship based on transfer function, linear, nonlinear, or continuous. It transforms the input by weights to find the relationships among neurons [103, 104, 105]. After developing the network topology, the network is trained. It can be trained through a supervised or unsupervised process, its prediction is validated and tested with a part of the training data.

ANNs have found uses in mechanical fatigue [106], including corrosion [107, 108], and is applicable to modulate the stochastic processes of temporal behavior as in offshore components [109, 110, 111]. [112] perform the fatigue assessment of floating wind turbines integrating environmental conditions using ANN approach. [113] incorporated the corrosion effect to propose a probabilistic solution of Paris' law [114] proposed to use a neural network to detect the damage in offshore jacket platforms. [39] evaluated the wellhead's fatigue life during service life using the dynamic Bayesian network. [115] predict the wind farm power structural fatigue. The offshore structure dynamic can be performed in the frequency or time domain. The former is faster, but the time domain includes the nonlinearities to reduce the variance. [116] used the neural network in the time domain to reduce the variance to predict the damage. [117] proposed a damage detection of offshore structures based on the vibration response; this was used as a damage indicator to get the location and its severity.

Also, ANN can be used to develop transfer functions that can be used to estimate the ocean current velocities along the length of the marine drilling riser [118] to evaluate the Flapwise Blade roof bending moments [119, 120]. [121] proposes the monitoring of human fatigue during a marine operation, ANN is used to maintain marine assets such as ship structures, offshore renewable energy platforms, and subsea oil and gas facilities [122]. A prediction approach based on a backpropagation neural network is proposed to evaluate the stress of floating, production, storage, and offloading (FPSO) units at different oil storage conditions [123, 124, 125].

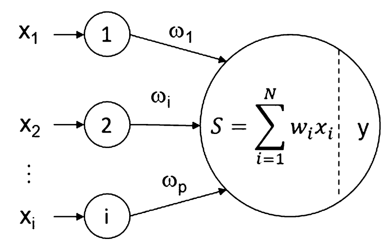

Fig. 14. Schematic representation of a neuron.

In the artificial neural network, the main components include inputs, outputs, weights, and activation functions [126]. The configuration of the network depends on the training sample number [127]. The neural network approach usually follows three steps: preparation of the database, design ANN topology, and training. In the training step, the training algorithms and parameters of the network are chosen.

NN can reproduce the behavior of complex nonlinear relationships by applying many nonlinear processing units, sometimes called neurons. A flow chart for a single neuron is shown in Fig. 14.

This neuron produces its output by combining the input signals and transforming it by a transfer function. Each hidden unit y_j sums its weighted input signal and applies a transfer function as is expressed by

$$y_j = f\left(\sum_{i=1}\omega_{ij}x_i + b_i\right) \tag{38}$$

where ω_{ij} is the weight from the connection between the input unit x_i to the hidden unit y_i and b_i is the bias, initially set to random values. The output signal of the hidden unit y_j is sent to all units in the next hidden or output layer. Each output unit o_k sums its weighted input signal and applies its transfer function to compute its output signal.

Back propagation (BP) is employed during training, this technique minimizes the error E for output neuron as follows

$$E = \frac{1}{2}\sum_{i=1}^{p}\sum_{k=1}^{k}\left(d_{pk} - o_{pk}\right)^2 \tag{39}$$

where d_{pk} is the desired output, o_{pk} is the predicted output. The process is developed adjusting the weights $\Delta\omega_{ij}$ and biases [128], as it is shown

$$\Delta\omega_{ij} = -\alpha\frac{2E}{\partial\omega_{ij}} + \beta\Delta\omega_{ij}(s-1) \tag{40}$$

This algorithm tries to overfit the data set, to prevent it, is used a regularization function as is shown in eq. (41)

$$F = \beta E_D + \alpha E_w, \quad E_w = \sum_{i=1}^{N} w_i^2 \tag{41}$$

where E_w is the sum of square errors of the ANN weights and α and β are objective function parameters. The weights are expressed by [129]

$$P(w|D,\alpha,\beta,M) = \frac{P(D,w,\beta,M)P(w|\alpha,M)}{P(D,\alpha,\beta,M)} \tag{42}$$

Considering that the noise is Gaussian in the input parameters of the network, the distributions of the weights are Gaussian

$$P(D|w,\beta,M) = \frac{1}{Z_D(\beta)}\exp(-\beta E_D) \tag{43}$$

$$P(w,\alpha,M) = \frac{1}{Z_w(\alpha)}\exp(-\alpha E_w) \tag{44}$$

where $Z_D(\beta) = (\frac{\pi}{\beta})^{\frac{n}{2}}$ and $Z_w(\alpha) = (\frac{pi}{\alpha})^{\frac{N}{2}}$.

Dynamic Bayesian Network (DBN) is an extension of BN, it can be expressed as a generalization of Markov process model. The conditional probability table for a set of stochastic variables X at each time step is then expressed as, $P\left(X^{i+1}\right)|X^{i},Pa\left(X^{i+1}\right),Pa\left(X^{i}\right)$ [121]. Finally, the joint distribution of a set of X random variables in $i+1$ time step as:

$$P\left(X^{i+1}\right)=\Pi_{j=1}^{m}\left(X_{j}^{i+1}\right)|X_{j}^{i},Pa\left(X_{j}^{i+1}\right),Pa\left(X_{j}^{i}\right)i=1,..n;j=1,..m \quad (45)$$

Radial basis function (RBF) normally represented by a Gaussian function by a center and width. The first layer weights are trained to perform a clustering of vectors, through Kohonen learning rule as:

$$i^{*}W^{1}(q)=i^{*}W^{1}(q-1)+\alpha\left(p(q)-i^{*}W^{1}(q-1)\right) \quad (46)$$

where $p(q)$ is one of the inputs vectors, $i^{*}W^{1}(q-1)$ is the closest weight to the input [103, 124].

Convolutional Neural Network used convolutional kernels to convolute the local area of the input [117, 130]. For time series value, o_i is the output of the convolutional layer i, which can be expressed as

$$O_i=f\left(O_{i-1}\times W_i+b\right) \quad (47)$$

where O_{i-1} is the output of the convolutional layer $i-1$.

General Regression Neural Network (GRNN) is built on the kernel regression Bayes decision to predict the joint probability density function. *Random Forest* (RF) is a regression approach for parametric and non-parametric classification. *Support Vector Machine* (SVM) helps to deal with complex systems and corrupted data; this is performed using the structural risk minimization to get the regression hyperplane through nonlinear transformation satisfying the Mercer's condition. *Gradient Boosting Regression* (GBR) is a prediction approach that combines machine learning and statistical boosting [131, 132, 133]. A *Recurrent Neural Network* (RNN) has feedback connections to perform the current prediction using the input data and the previous outputs; this can generate large or small gradients [134, 135]. To manage this issue, *Long Short Term Memory* (LSTM) cells are a designed fate memory with internal mechanics known as gates to regulate the gradients of information flow [115]. Hierarchical models are an effective way of representing systems whose characteristics can be grouped using multiple levels [107].

5. Summary

Fatigue life prediction in maritime areas such as harbor and coastal structures is necessary to prevent unexpected failures. These structures are near located the coast and on the coast, and there is a connection between the sea and the land. The source of loads is mainly the wind and water. It is thus necessary to understand the movement of the water in waves, which can be represented by a sinusoidal waveform. However, its movement is not constant, and depends on natural factors, temperatures, tidal effects, and moon effects. In addition to these variables, there are extreme conditions such as typhoons that can increase the intensity of the loads. Although methods have been proposed to perform fatigue prediction with correction factors, the dispersion associated with fatigue still requires experimental tests to include the effects of temperature, overload and corrosion. There are corrosion protection methods, however they can be damaged by impact. Additionally, there are factors such as the variability in loads that can be considered as deterministic assumptions to analyze the structures. However, in this case, it is necessary to analyze it as probabilistic due to random processes. Is mandatory ascertaining the durability of marine structures as harbor and coastal structures to prevent overdesign and obtain information on environmental effects and type of random variables, such as wind, wave loads, ice, and corrosion effects. To propose new linear or analytical tools, numerical tools can be evaluated to be used as a nonlinear option to predict the fatigue life; however, it is mandatory to conduct training in a long-term process. Highly overstressed situations and typhoons can be trained based on previous phenomena in different places. An additional advantage is that ANN can be used for monitoring during the service life as a nondestructive tool for analysis with a digital twin, it can detect any change in material strength during an acceleration damage process for corrosion, and can identify requirements for maintenance or repairs. Although neural networks are highly adaptable to non-linear systems, such as random loads, and the consideration of environmental effects obtained from experimental tests or monitored data, one of their limitations is the validation only in training ranges.

Declarations

Author contribution statement

All authors listed have significantly contributed to the development and the writing of this article.

Funding statement

This research did not receive any specific grant from funding agencies in the public, commercial, or not-for-profit sectors.

Data availability statement

No data was used for the research described in the article

Declaration of interests statement

The authors declare no conflict of interest.

Additional information

No additional information is available for this paper.

References

[1] P.K. Stansby, Coastal hydrodynamics – present and future, J. Hydraul. Res. 51 (4) (2013) 341–350.
[2] A. Hildebrandt, B. Schmidt, S. Marx, Wind-wave misalignment and a combination method for direction-dependent extreme incidents, Ocean Eng. 180 (2019) 10–22.
[3] I. Thompson, Fatigue damage variation within a class of naval ships, Ocean Eng. 165 (2018) 123–130.
[4] J. Zhu, W. Zhang, Probabilistic fatigue damage assessment of coastal slender bridges under coupled dynamic loads, Eng. Struct. 166 (2018) 274–285.
[5] S.-H. Yang, J.W. Ringsberg, E. Johnson, Z. Hu, J. Palm, A comparison of coupled and de-coupled simulation procedures for the fatigue analysis of wave energy converter mooring lines, Ocean Eng. 117 (2016) 332–345.
[6] J. Pokhrel, J. Seo, Natural hazard vulnerability quantification of offshore wind turbine in shallow water, Eng. Struct. 192 (2019) 254–263.
[7] Z.-Y. Wang, F. Yuan, Y. Chen, Q. Wang, T. Chen, X. Zhou, Z. Liu, Fatigue resistance of post-buckled slender trapezoidal corrugated webs in girders with stiff flanges, Eng. Struct. 198 (2019) 109478.
[8] P. Jonathan, K. Ewans, J. Flynn, Joint modelling of vertical profiles of large ocean currents, Ocean Eng. 42 (2012) 195–204.
[9] B. Gaspar, A. Teixeira, C. Guedes Soares, Effect of the nonlinear vertical wave-induced bending moments on the ship hull girder reliability, Ocean Eng. 119 (2016) 193–207.
[10] J. Kam, Recent development in the fast corrosion fatigue analysis of offshore structures subject to random wave loading, Int. J. Fatigue 12 (6) (1990) 458–468.
[11] C. Sun, V. Jahangiri, Fatigue damage mitigation of offshore wind turbines under real wind and wave conditions, Eng. Struct. 178 (2019) 472–483.
[12] P. Jonathan, K. Ewans, Statistical modelling of extreme ocean environments for marine design: a review, Ocean Eng. 62 (2013) 91–109.
[13] W. Cui, F. Wang, X. Huang, A unified fatigue life prediction method for marine structures, Mar. Struct. 24 (2) (2011) 153–181.
[14] R. Perveen, N. Kishor, S.R. Mohanty, Off-shore wind farm development: present status and challenges, Renew. Sustain. Energy Rev. 29 (2014) 780–792.
[15] B.M. Sumer, Flow–structure–seabed interactions in coastal and marine environments, J. Hydraul. Res. 52 (1) (2014) 1–13.
[16] D.J. Tong, Y.M. Low, J.M. Sheehan, Nonlinear bend stiffener analysis using a simple formulation and finite element methods, China Ocean Eng. 25 (2011) 577–590.
[17] R. Chen, Y.M. Low, Efficient long-term fatigue analysis of deepwater risers in the time domain including wave directionality, Mar. Struct. 78 (2021) 103002.
[18] Z. Zhao, K. Dai, E.R. Lalonde, J. Meng, B. Li, Z. Ding, G. Bitsuamlak, Studies on application of scissor-Jack braced viscous damper system in wind turbines under seismic and wind loads, Eng. Struct. 196 (2019) 109294.
[19] P.-Y. Le Gac, M. Arhant, P. Davies, A. Muhr, Fatigue behavior of natural rubber in marine environment: comparison between air and sea water, in: Materials & Design (1980-2015), vol. 65, 2015, pp. 462–467.

[20] W. Yuan, A. Guo, H. Li, Seismic failure mode of coastal bridge piers considering the effects of corrosion-induced damage, Soil Dyn. Earthq. Eng. 93 (2017) 135–146.
[21] E. Poursaeidi, A. Babaei, F. Behrouzshad, M. Mohammadi Arhani, Failure analysis of an axial compressor first row rotating blades, Eng. Fail. Anal. 28 (2013) 25–33.
[22] S. Zhang, T. Zhang, Y. He, Y. Feng, X. Du, B. Ma, T. Zhang, Effect of coastal atmospheric corrosion on fatigue properties of 2024-t4 aluminum alloy structures, J. Alloys Compd. 802 (2019) 511–521.
[23] J. Du, H. Wang, S. Wang, X. Song, J. Wang, A. Chang, Fatigue damage assessment of mooring lines under the effect of wave climate change and marine corrosion, Ocean Eng. 206 (2020) 107303.
[24] W. Khodabux, C. Liao, F. Brennan, Characterisation of pitting corrosion for inner section of offshore wind foundation using laser scanning, Ocean Eng. 230 (2021) 109079.
[25] T. Palin-Luc, R. Pérez-Mora, C. Bathias, G. Domínguez, P.C. Paris, J.L. Arana, Fatigue crack initiation and growth on a steel in the very high cycle regime with sea water corrosion, in: International Conference on Crack Paths 2009, Eng. Fract. Mech. 77 (11) (2010) 1953–1962.
[26] M.A.C. Gonzales, P. Kujala, Additive manufacturing of miniature marine structures for crashworthiness verification: a numerical revision, Appl. Ocean Res. 111 (2021) 102653.
[27] T. Pire, H. Le Sourne, S. Echeverry, P. Rigo, Analytical formulations to assess the energy dissipated at the base of an offshore wind turbine jacket impacted by a ship, Mar. Struct. 59 (2018) 192–218.
[28] P. Hogström, J.W. Ringsberg, Assessment of the crashworthiness of a selection of innovative ship structures, Ocean Eng. 59 (2013) 58–72.
[29] A. Rio Prabowo, D. Myung Bae, J. Min Sohn, A. Fauzan Zakki, B. Cao, J. Hyung Cho, Effects of the rebounding of a striking ship on structural crashworthiness during ship-ship collision, Thin-Walled Struct. 115 (2017) 225–239.
[30] J. Wang, Y. Song, W. Wang, L. Tu, Evaluation of composite crashworthy device for pier protection against barge impact, Ocean Eng. 169 (2018) 144–158.
[31] P. Kaczyński, M. Ptak, K. Gawdzińska, Energy absorption of cast metal and composite foams tested in extremely low and high-temperatures, Mater. Des. 196 (2020) 109114.
[32] C. Liu, E. Hao, S. Zhang, Optimization and application of a crashworthy device for the monopile offshore wind turbine against ship impact, Appl. Ocean Res. 51 (2015) 129–137.
[33] M. Horstmann, J. Gregory, K.-H. Schwalbe, Geometry effects on corrosion-fatigue in offshore structural steels, Int. J. Fatigue 17 (4) (1995) 293–299.
[34] A. Mehmanparast, A. Vidament, An accelerated corrosion-fatigue testing methodology for offshore wind applications, Eng. Struct. 240 (2021) 112414.
[35] C. Lindley, W.J. Rudd, Influence of the level of cathodic protection on the corrosion fatigue properties of high-strength welded joints, Mar. Struct. 14 (4) (2001) 397–416. Jack-up Platforms.
[36] O. Adedipe, F. Brennan, A. Kolios, Corrosion fatigue load frequency sensitivity analysis, Mar. Struct. 42 (2015) 115–136.
[37] O. Adedipe, F. Brennan, A. Kolios, Review of corrosion fatigue in offshore structures: present status and challenges in the offshore wind sector, Renew. Sustain. Energy Rev. 61 (2016) 141–154.
[38] A. Cheng, N.-Z. Chen, An extended engineering critical assessment for corrosion fatigue of subsea pipeline steels, Eng. Fail. Anal. 84 (2018) 262–275.
[39] Y. Chang, X. Wu, C. Zhang, G. Chen, X. Liu, J. Li, B. Cai, L. Xu, Dynamic Bayesian networks based approach for risk analysis of subsea wellhead fatigue failure during service life, Reliab. Eng. Syst. Saf. 188 (2019) 454–462.
[40] T.A. Piedras Lopes, N.F. Ebecken, In-time fatigue monitoring using neural networks, Mar. Struct. 10 (5) (1997) 363–387.
[41] L. Sun, C. Liu, Z. Zong, X. Dong, Fatigue damage analysis of the deepwater riser from viv using pseudo-excitation method, Mar. Struct. 37 (2014) 86–110.
[42] H.-J. Kim, B.-S. Jang, C.-K. Park, Y.H. Bae, Fatigue analysis of floating wind turbine support structure applying modified stress transfer function by artificial neural network, Ocean Eng. 149 (2018) 113–126.
[43] M. Machado, A. Appert, L. Khalij, Spectral formulated modelling of an electrodynamic shaker, Mech. Res. Commun. 97 (2019) 70–78.
[44] Q.A. Mai, W. Weijtjens, C. Devriendt, P.G. Morato, P. Rigo, J.D. Sørensen, Prediction of remaining fatigue life of welded joints in wind turbine support structures considering strain measurement and a joint distribution of oceanographic data, Mar. Struct. 66 (2019) 307–322.
[45] M. Storheim, J. Amdahl, I. Martens, On the accuracy of fracture estimation in collision analysis of ship and offshore structures, Mar. Struct. 44 (2015) 254–287.
[46] P. Kumar, H. Zhang, K. Ik Kim, D.A. Yuen, Modeling wave and spectral characteristics of moored ship motion in pohang new harbor under the resonance conditions, Ocean Eng. 119 (2016) 101–113.
[47] J.W. Kamphuis, Introduction to Coastal Engineering and Management, World Scientific, 2010.
[48] E.M. Bitner-Gregersen, S. Dong, T. Fu, N. Ma, C. Maisondieu, R. Miyake, I. Rychlik, Sea state conditions for marine structures' analysis and model tests, Ocean Eng. 119 (2016) 309–322.
[49] C. Larsen, L. Lutes, Predicting the fatigue life of offshore structures by the single-moment spectral method, Probab. Eng. Mech. 6 (2) (1991) 96–108.
[50] C.E. Larsen, T. Irvine, A review of spectral methods for variable amplitude fatigue prediction and new results, in: 3rd International Conference on Material and Component Performance Under Variable Amplitude Loading, VAL 2015, in: Procedia Engineering, vol. 101, 2015, pp. 243–250.
[51] T. Dirlik, D. Benasciutti, Dirlik and tovo-benasciutti spectral methods in vibration fatigue: a review with a historical perspective, Metals 11 (9) (2021).
[52] K. Tran Nguyen, Y. Garbatov, C. Guedes Soares, Spectral fatigue damage assessment of tanker deck structural detail subjected to time-dependent corrosion, Int. J. Fatigue 48 (2013) 147–155.
[53] P. Shabani, F. Taheri-Behrooz, S.S. Samareh-Mousavi, M.M. Shokrieh, Very high cycle and gigacycle fatigue of fiber-reinforced composites: a review on experimental approaches and fatigue damage mechanisms, Prog. Mater. Sci. 118 (2021) 100762.
[54] P. Les, Metal Fatigue, Springer, Netherlands, 2007.
[55] E. Homaei, K. Farhangdoost, J.K.H. Tsoi, J.P. Matinlinna, E.H.N. Pow, Static and fatigue mechanical behavior of three dental cad/cam ceramics, J. Mech. Behav. Biomed. Mater. 59 (2016) 304–313.
[56] Y. Zhao, S. Dong, Probabilistic fatigue surrogate model of bimodal tension process for a semi-submersible platform, Ocean Eng. 220 (2021) 108501.
[57] M. Jimenez-Martinez, Manufacturing effects on fatigue strength, Eng. Fail. Anal. 108 (2020) 104339.
[58] W. Yonglian, A generalized frequency modified damage function model for high temperature low cycle fatigue life prediction, Int. J. Fatigue 19 (4) (1997) 345–350.
[59] L. Pazos, P. Corengia, H. Svoboda, Effect of surface treatments on the fatigue life of titanium for biomedical applications, J. Mech. Behav. Biomed. Mater. 3 (6) (2010) 416–424.
[60] T. Palin-Luc, D. Jeddi, The gigacycle fatigue strength of steels: a review of structural and operating factors, in: eCF22 - Loading and Environmental Effects on Structural Integrity, in: Procedia Structural Integrity, vol. 13, 2018, pp. 1545–1553.
[61] R. Morrissey, T. Nicholas, Staircase testing of a titanium alloy in the gigacycle regime, in: Third International Conference on Very High Cycle Fatigue (VHCF-3), Int. J. Fatigue 28 (11) (2006) 1577–1582.
[62] S. Stanzl-Tschegg, Very high cycle fatigue measuring techniques, Int. J. Fatigue 60 (2014) 2–17. New Advances in VHCF.
[63] C. Sonsino, Multiaxial fatigue life response depending on proportionality grade between normal and shear strains/stresses and material ductility, Int. J. Fatigue 135 (2020) 105468.
[64] Z.Y. Huang, H.Q. Liu, H.M. Wang, D. Wagner, M.K. Khan, Q.Y. Wang, Effect of stress ratio on vhcf behavior for a compressor blade titanium alloy, Int. J. Fatigue 93 (2016) 232–237. Gigacycle Fatigue-Theory and Applications Dedicated to the Memory of Professor Claude Bathias.
[65] Z.Y. Huang, H.Q. Liu, H.M. Wang, D. Wagner, M.K. Khan, Q.Y. Wang, Effect of stress ratio on vhcf behavior for a compressor blade titanium alloy, Int. J. Fatigue 93 (2016) 232–237. Gigacycle Fatigue-Theory and Applications Dedicated to the Memory of Professor Claude Bathias.
[66] A. Zalaznik, M. Nagode, Frequency based fatigue analysis and temperature effect, Mater. Des. 32 (10) (2011) 4794–4802.
[67] R. Ebara, The present situation and future problems in ultrasonic fatigue testing – mainly reviewed on environmental effects and materials' screening, in: Third International Conference on Very High Cycle Fatigue (VHCF-3), Int. J. Fatigue 28 (11) (2006) 1465–1470.
[68] D.V. Osti de Moraes, R. Magnabosco, G.H. Bolognesi Donato, S.H. Prado Bettini, M.C. Antunes, Influence of loading frequency on the fatigue behaviour of coir fibre reinforced pp composite, Polym. Test. 41 (2015) 184–190.
[69] B. Zettl, H. Mayer, S. Stanzl-Tschegg, Fatigue properties of al–1mg–0.6si foam at low and ultrasonic frequencies, Int. J. Fatigue 23 (7) (2001) 565–573.
[70] E. Takeuchi, Y. Furuya, N. Nagashima, S. Matsuoka, The effect of frequency on the giga-cycle fatigue properties of a ti–6al–4v alloy, Fatigue Fract. Eng. Mater. Struct. 31 (2008) 599–605.
[71] Y. Furuya, S. Matsuoka, T. Abe, K. Yamaguchi, Gigacycle fatigue properties for high-strength low-alloy steel at 100 hz, 600 hz, and 20 khz, Scr. Mater. 46 (2) (2002) 157–162.
[72] O. Costa Garrido, S. El Shawish, L. Cizelj, Uncertainties in the thermal fatigue assessment of pipes under turbulent fluid mixing using an improved spectral loading approach, Int. J. Fatigue 82 (2016) 550–560.
[73] Y. Baik, K. Kim, The combined effect of frequency and load level on fatigue crack growth in stainless steel 304, Int. J. Fatigue 23 (5) (2001) 417–425.
[74] M. Kawai, Y. Ishizuka, Fatigue life of woven fabric carbon/epoxy laminates under alternating r-ratio loading along non-proportional path in the σm-σa plane, Int. J. Fatigue 112 (2018) 36–51.
[75] M. Fitzka, H. Mayer, Constant and variable amplitude fatigue testing of aluminum alloy 2024-t351 with ultrasonic and servo-hydraulic equipment, Int. J. Fatigue 91 (2016) 363–372. Variable Amplitude Loading.
[76] A. Audenino, V. Crupi, E. Zanetti, Correlation between thermography and internal damping in metals, Int. J. Fatigue 25 (4) (2003) 343–351.
[77] R. Arone, Application of wheeler retardation model for assessment of fatigue crack lifetime under random overloads, Int. J. Fatigue 12 (4) (1990) 275–281.
[78] J. Treadway, A. Abolmaali, F. Lu, P. Aswath, Tensile and fatigue behavior of superelastic shape memory rods, Mater. Des. 86 (2015) 105–113.
[79] Z. Li dong, S. tong Zhou, C. fu Yang, Q. long Yong, High/very high cycle fatigue behaviors of medium carbon pearlitic wheel steels and the effects of microstructure and non-metallic inclusions, Mater. Sci. Eng. A 764 (2019) 138208.

[80] P. Reis, J. Monteiro, A. Pereira, J. Ferreira, J. Costa, Fatigue behaviour of epoxy-steel single lap joints under variable frequency, Int. J. Adhes. Adhes. 63 (2015) 66–73.
[81] D. Hülsbusch, A. Kohl, P. Striemann, M. Niedermeier, J. Strauch, F. Walther, Development of an energy-based approach for optimized frequency selection for fatigue testing on polymers – exemplified on polyamide 6, Polym. Test. 81 (2020) 106260.
[82] N. Marti, V. Favier, F. Gregori, N. Saintier, Correlation of the low and high frequency fatigue responses of pure polycrystalline copper with mechanisms of slip band formation, Mater. Sci. Eng. A 772 (2020) 138619.
[83] M. Izadi, E. Ghafoori, M. Motavalli, S. Maalek, Iron-based shape memory alloy for the fatigue strengthening of cracked steel plates: effects of re-activations and loading frequencies, Eng. Struct. 176 (2018) 953–967.
[84] M.-L. Zhu, L.-L. Liu, F.-Z. Xuan, Effect of frequency on very high cycle fatigue behavior of a low strength cr–ni–mo–v steel welded joint, Int. J. Fatigue 77 (2015) 166–173.
[85] R. Zeng, E. Han, W. Ke, A critical discussion on influence of loading frequency on fatigue crack propagation behavior for extruded mg–al–zn alloys, Int. J. Fatigue 36 (1) (2012) 40–46.
[86] I. Nikitin, M. Besel, Effect of low-frequency on fatigue behaviour of austenitic steel aisi 304 at room temperature and 25°C, Int. J. Fatigue 30 (10) (2008) 2044–2049.
[87] L. Li, X. Gu, S. Sun, W. Wang, Z. Wan, P. Qian, Effects of welding residual stresses on the vibration fatigue life of a ship's shock absorption support, Ocean Eng. 170 (2018) 237–245.
[88] L. Feng, L. Zhang, X. Liao, W. Zhang, Probabilistic fatigue life of welded plate joints under uncertainty in Arctic areas, J. Constr. Steel Res. 176 (2021) 106412.
[89] W. Barrois, Repeated plastic deformation as a cause of mechanical surface damage in fatigue, wear, fretting-fatigue, and rolling fatigue: a review, Int. J. Fatigue 1 (4) (1979) 167–189.
[90] W. Zhao, M.J. Baker, On the probability density function of rainflow stress range for stationary Gaussian processes, Int. J. Fatigue 14 (2) (1992) 121–135.
[91] X. Liu, C. Sun, Y. Hong, Effects of stress ratio on high-cycle and very-high-cycle fatigue behavior of a ti–6al–4v alloy, Mater. Sci. Eng. A 622 (2015) 228–235.
[92] W. Schütz, The prediction of fatigue life in the crack initiation and propagation stages—a state of the art survey, Eng. Fract. Mech. 11 (2) (1979) 405–421.
[93] B. Guennec, A. Ueno, T. Sakai, M. Takanashi, Y. Itabashi, Effect of the loading frequency on fatigue properties of jis s15c low carbon steel and some discussions based on micro-plasticity behavior, Int. J. Fatigue 66 (2014) 29–38.
[94] S. Stanzl-Tschegg, H. Mayer, E. Tschegg, High frequency method for torsion fatigue testing, Ultrasonics 31 (4) (1993) 275–280.
[95] H. Schechtman, D. Bader, Fatigue damage of human tendons, J. Biomech. 35 (3) (2002) 347–353.
[96] O. Kovářík, P. Haušild, J. Čapek, J. Medřický, J. Siegl, R. Mušálek, Z. Pala, N. Curry, S. Björklund, Resonance bending fatigue testing with simultaneous damping measurement and its application on layered coatings, in: 10th Fatigue Damage of Structural Materials Conference, Int. J. Fatigue 82 (2016) 300–309.
[97] M. Bonte, A. de Boer, R. Liebregts, Determining the von Mises stress power spectral density for frequency domain fatigue analysis including out-of-phase stress components, J. Sound Vib. 302 (1) (2007) 379–386.
[98] A. Carpinteri, A. Spagnoli, S. Vantadori, A review of multiaxial fatigue criteria for random variable amplitude loads, Fatigue Fract. Eng. Mater. Struct. 40 (7) (2017) 1007–1036.
[99] Y.-L. Lee, 10-fatigue analysis in the frequency domain, in: Y.-L. Lee, J. Pan, R.B. Hathaway, M.E. Barkey (Eds.), Fatigue Testing and Analysis, Butterworth-Heinemann, Burlington, 2005, pp. 369–394.
[100] L. Meirovitch, Elements of Vibration Analysis, McGraw-Hill Science/Engineering/Math, 1986.
[101] T. Dirlik, Application of Computers in Fatigue Analysis, PhD thesis submitted to Engineering Department, University of Warwick, 1985.
[102] Y. Li, B.J. Lence, Z. Shi-Liang, Q. Wu, Stochastic fatigue assessment for berthing monopiles in inland waterways, J. Waterw. Port Coast. Ocean Eng. 137 (2) (2011) 43–53.
[103] A. Fathi, A. Aghakouchak, Prediction of fatigue crack growth rate in welded tubular joints using neural network, Int. J. Fatigue 29 (2) (2007) 261–275.
[104] M.H. Shojaeefard, R.A. Behnagh, M. Akbari, M.K.B. Givi, F. Farhani, Modelling and Pareto optimization of mechanical properties of friction stir welded aa7075/aa5083 butt joints using neural network and particle swarm algorithm, Mater. Des. 44 (2013) 190–198.
[105] J. Durodola, N. Li, S. Ramachandra, A. Thite, A pattern recognition artificial neural network method for random fatigue loading life prediction, Int. J. Fatigue 99 (2017) 55–67.
[106] P. Orbanić, M. Fajdiga, A neural network approach to describing the fretting fatigue in aluminium-steel couplings, Int. J. Fatigue 25 (3) (2003) 201–207.
[107] J. Luque, D. Straub, Reliability analysis and updating of deteriorating systems with dynamic Bayesian networks, Struct. Saf. 62 (2016) 34–46.
[108] X. Zhao, D. Ru, P. Wang, L. Gan, H. Wu, Z. Zhong, Fatigue life prediction of a supercritical steam turbine rotor based on neural networks, Eng. Fail. Anal. (2021) 105435.
[109] E. Arzaghi, M.M. Abaei, R. Abbassi, V. Garaniya, C. Chin, F. Khan, Risk-based maintenance planning of subsea pipelines through fatigue crack growth monitoring, Eng. Fail. Anal. 79 (2017) 928–939.
[110] H.-J. Kim, B.-S. Jang, C.-K. Park, Y.H. Bae, Fatigue analysis of floating wind turbine support structure applying modified stress transfer function by artificial neural network, Ocean Eng. 149 (2018) 113–126.
[111] M. Martinez-Luengo, M. Shafiee, A. Kolios, Data management for structural integrity assessment of offshore wind turbine support structures: data cleansing and missing data imputation, Ocean Eng. 173 (2019) 867–883.
[112] X. Li, W. Zhang, Long-term fatigue damage assessment for a floating offshore wind turbine under realistic environmental conditions, Renew. Energy 159 (2020) 570–584.
[113] L. Chen, E. Arzaghi, M.M. Abaei, V. Garaniya, R. Abbassi, Condition monitoring of subsea pipelines considering stress observation and structural deterioration, J. Loss Prev. Process Ind. 51 (2018) 178–185.
[114] A.A. Elshafey, M.R. Haddara, H. Marzouk, Damage detection in offshore structures using neural networks, Mar. Struct. 23 (1) (2010) 131–145.
[115] X. Yin, X. Zhao, Big data driven multi-objective predictions for offshore wind farm based on machine learning algorithms, Energy 186 (2019) 115704.
[116] R. Chen, Y.M. Low, Reducing uncertainty in time domain fatigue analysis of offshore structures using control variates, Mech. Syst. Signal Process. 149 (2021) 107192.
[117] X. Bao, T. Fan, C. Shi, G. Yang, One-dimensional convolutional neural network for damage detection of jacket-type offshore platforms, Ocean Eng. 219 (2021) 108293.
[118] J. Seifert, L. Vera-Tudela, M. Kühn, Training requirements of a neural network used for fatigue load estimation of offshore wind turbines, in: 14th Deep Sea Offshore Wind R&D Conference, EERA DeepWind'2017, Energy Proc. 137 (2017) 315–322.
[119] K. Müller, M. Dazer, P.W. Cheng, Damage assessment of floating offshore wind turbines using response surface modeling, in: 14th Deep Sea Offshore Wind R&D Conference, EERA DeepWind'2017, Energy Proc. 137 (2017) 119–133.
[120] S. Liu, J. Guzzo, L. Zhang, U. Kumar, G.J. Myers, Ultra-deepwater drilling riser lifecycle management system, in: Proceedings of the 8th International Conference on Through-Life Engineering Services, TESConf 2019, in: Procedia Manufacturing, vol. 49, 2020, pp. 211–216.
[121] M.M. Abaei, R. Abbassi, V. Garaniya, E. Arzaghi, A. Bahoo Toroody, A dynamic human reliability model for marine and offshore operations in harsh environments, Ocean Eng. 173 (2019) 90–97.
[122] M. Abbas, M. Shafiee, An overview of maintenance management strategies for corroded steel structures in extreme marine environments, Mar. Struct. 71 (2020) 102718.
[123] L. Wu, Y. Yang, M. Maheshwari, Strain prediction for critical positions of fpso under different loading of stored oil using gaifoa-bp neural network, Mar. Struct. 72 (2020) 102762.
[124] H. Rezaniaiee Aqdam, M.M. Ettefagh, R. Hassannejad, Health monitoring of mooring lines in floating structures using artificial neural networks, Ocean Eng. 164 (2018) 284–297.
[125] C.B. Li, J. Choung, M.-H. Noh, Wide-banded fatigue damage evaluation of catenary mooring lines using various artificial neural networks models, Mar. Struct. 60 (2018) 186–200.
[126] T. Varol, A. Canakci, S. Ozsahin, Artificial neural network modeling to effect of reinforcement properties on the physical and mechanical properties of al2024–b4c composites produced by powder metallurgy, Composites, Part B, Eng. 54 (2013) 224–233.
[127] G. zheng Quan, W. quan Lv, Y. ping Mao, Y. wei Zhang, J. Zhou, Prediction of flow stress in a wide temperature range involving phase transformation for as-cast ti–6al–2zr–1mo–1v alloy by artificial neural network, Mater. Des. 50 (2013) 51–61.
[128] A. Khan, M.H. Shamsi, T.-S. Choi, Correlating dynamical mechanical properties with temperature and clay composition of polymer-clay nanocomposites, Comput. Mater. Sci. 45 (2) (2009) 257–265.
[129] P. Kumar, S. Merchant, U.B. Desai, Improving performance in pulse radar detection using Bayesian regularization for neural network training, Digit. Signal Process. 14 (5) (2004) 438–448.
[130] H. Alqahtani, S. Bharadwaj, A. Ray, Classification of fatigue crack damage in polycrystalline alloy structures using convolutional neural networks, Eng. Fail. Anal. 119 (2021) 104908.
[131] X. Ma, X. He, Z. Tu, Prediction of fatigue–crack growth with neural network-based increment learning scheme, Eng. Fract. Mech. 241 (2021) 107402.
[132] L. He, Z. Wang, H. Akebono, A. Sugeta, Machine learning-based predictions of fatigue life and fatigue limit for steels, J. Mater. Sci. Technol. 90 (2021) 9–19.
[133] J. Chen, Y. Liu, Probabilistic physics-guided machine learning for fatigue data analysis, Expert Syst. Appl. 168 (2021) 114316.
[134] X.-C. Zhang, J.-G. Gong, F.-Z. Xuan, A deep learning based life prediction method for components under creep, fatigue and creep-fatigue conditions, Int. J. Fatigue 148 (2021) 106236.
[135] A. Paral, D.K. Singha Roy, A.K. Samanta, A deep learning-based approach for condition assessment of semi-rigid joint of steel frame, J. Build. Eng. 34 (2021) 101946.